# Star-in-a-box simulations of fully and partially convective stars

Petri J. Käpylä

Institute for Astrophysics, Göttingen University

Käpylä (2021), *A&A* (in press), arXiv:2012.01259

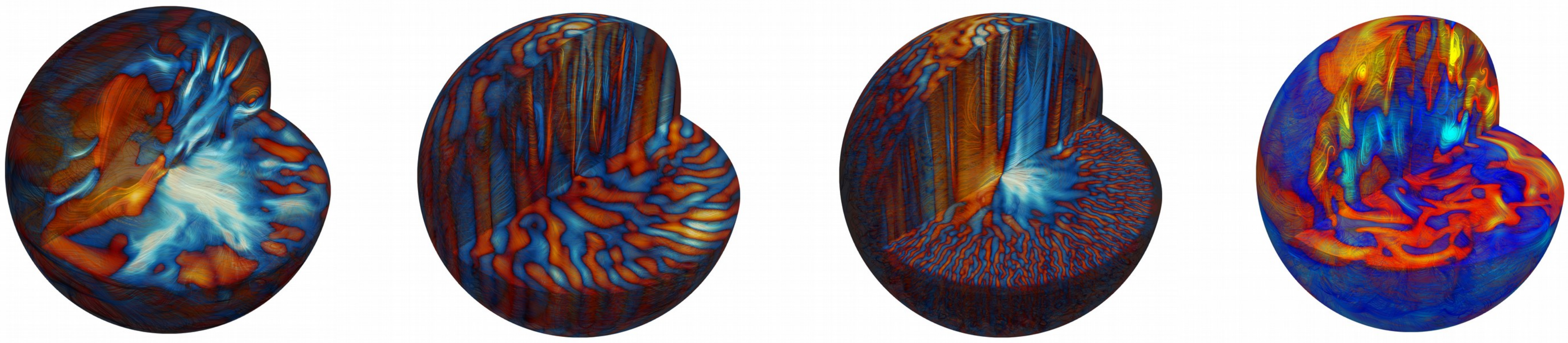

Pencil Code User Meeting 20 May 2021

# Introduction

Convective core

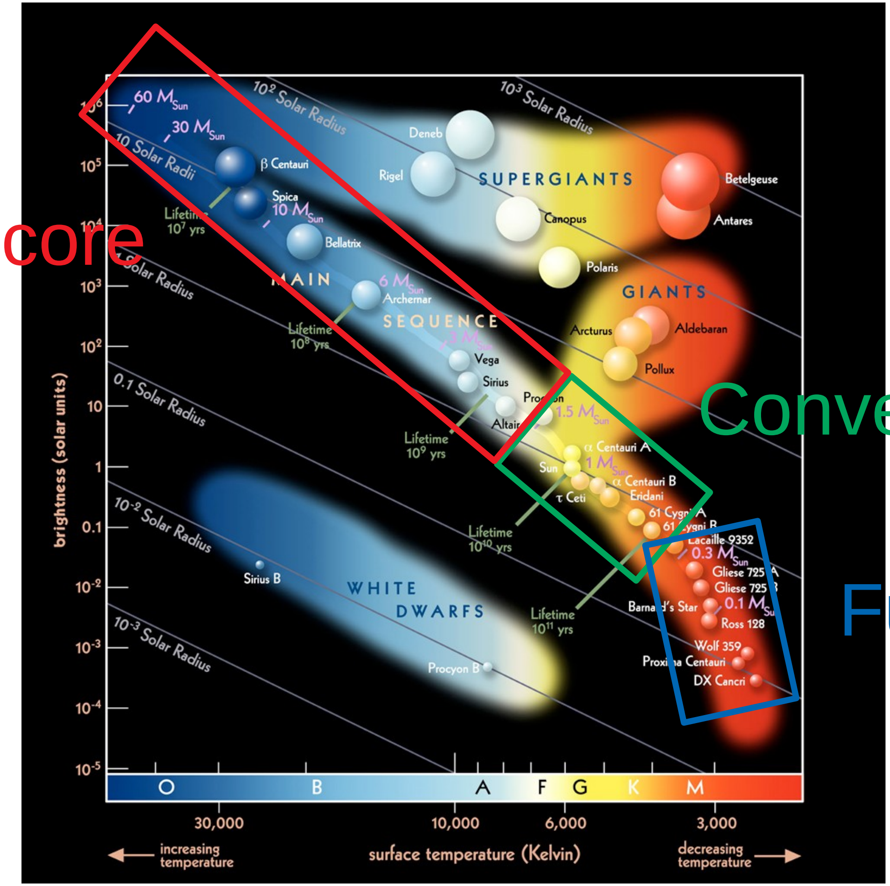


Convective envelope

Fully convective

# Polarized view on dynamos

No radiative zone → no tachocline: qualitatively different dynamo (and activity level?) than in the Sun?

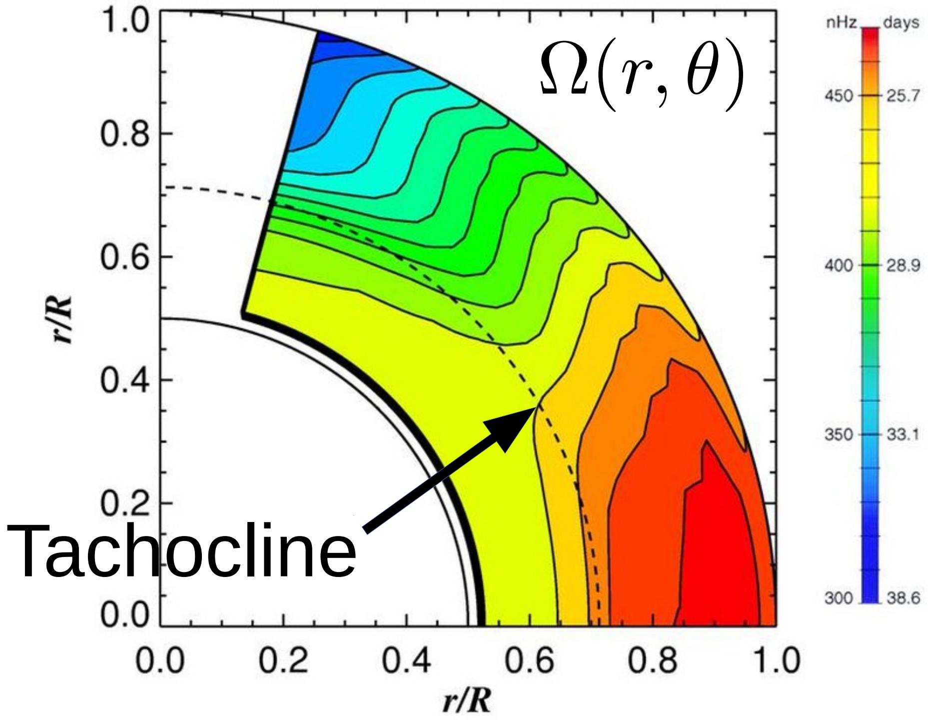


Flux transport dynamo: $\overline{B}_{\rm tor}$ due to shear in tachocline, $\overline{B}_{\rm pol}$ due to buoyant flux tubes. Convection unimportant.

Distributed dynamo: $\overline{\boldsymbol{B}}$ due to helical convection in CZ, shear in CZ contributes to $\overline{B}_{\rm tor}$. Tachocline unimportant.

# Implications for dynamos

Discontinuity in stellar structure at the transition: break in activity?

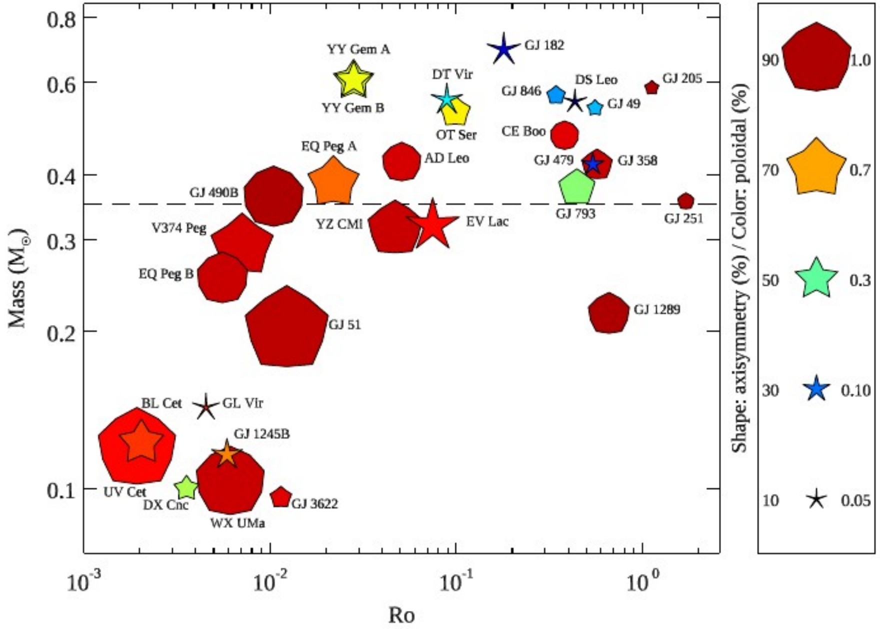


Kochukhov (2021), *Ann. Rev. Astron. Astrophys.*, **29**, 1

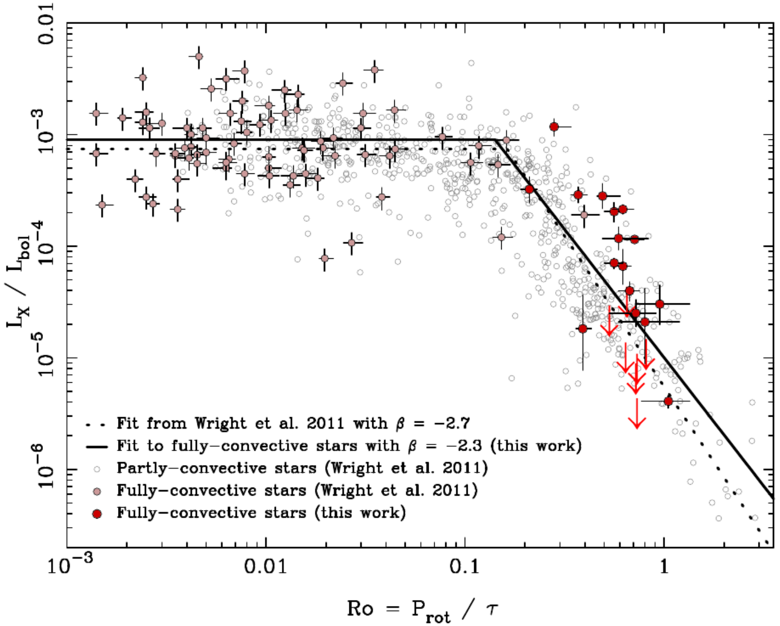


Wright et al. (2018), *MNRAS*, **479**, 2351

# Numerical modeling

Star-in-a-box model: embed a spherical star within a cube.

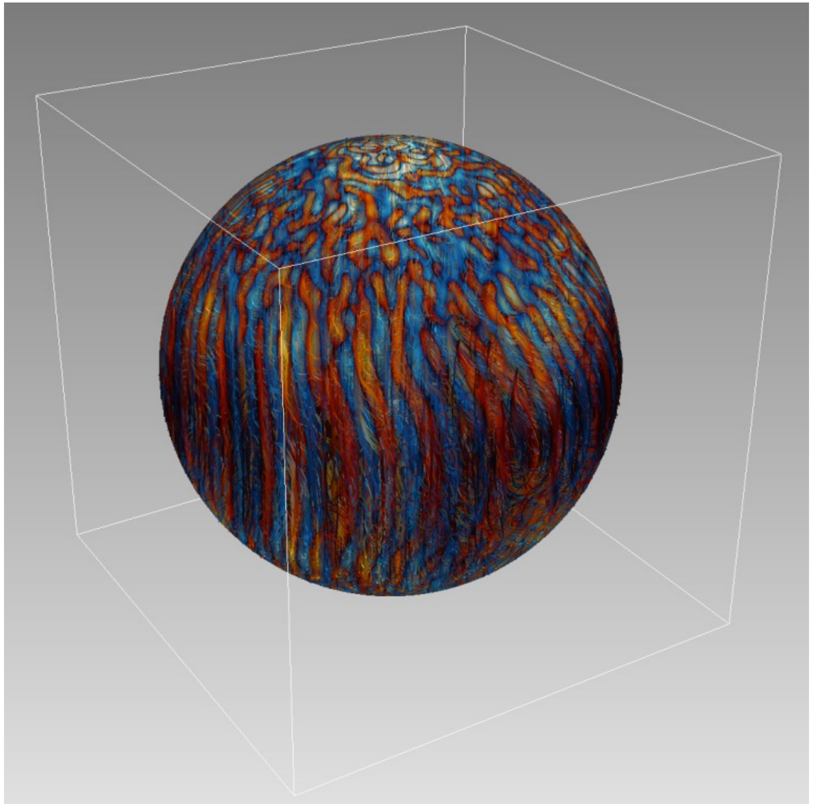

$$\frac{\partial \boldsymbol{A}}{\partial t} = \boldsymbol{U} \times \boldsymbol{B} - \eta\mu_0 \boldsymbol{J},$$

$$\frac{D\ln\rho}{Dt} = -\boldsymbol{\nabla}\cdot\boldsymbol{U},$$

$$\frac{D\boldsymbol{u}}{Dt} = -\boldsymbol{\nabla}\Phi - \frac{1}{\rho}(\boldsymbol{\nabla}p - \boldsymbol{\nabla}\cdot 2\nu\rho\mathbf{S} + \boldsymbol{J}\times\boldsymbol{B}) - 2\,\boldsymbol{\Omega}\times\boldsymbol{U} + \boldsymbol{f}_d,$$

$$T\frac{Ds}{Dt} = -\frac{1}{\rho}\left[\boldsymbol{\nabla}\cdot(\boldsymbol{F}_{\rm rad} + \boldsymbol{F}_{\rm SGS}) + \mathcal{H} - \mathcal{C}\right] + 2\nu\mathbf{S}^2 + \mu_0\eta\boldsymbol{J}^2,$$

Modestly updated version of the model of Dobler et al. (2006), *Astrophys. J.*, **638**, 336.

# Numerical modeling

Some salient features:

$$\boldsymbol{f}_{\rm d} = -\frac{\boldsymbol{U}}{\tau_{\rm damp}} f_e(r).$$

Velocity damping outside the star

$$\mathcal{H}(r) = \frac{L}{(2\pi w_l^2)^{3/2}} \exp\left(-\frac{r^2}{2w_L^2}\right).$$

Heating near the centre

$$\mathcal{C}(\boldsymbol{x}) = \rho c_{\rm P} \frac{T(\boldsymbol{x}) - T_{\rm surf}}{\tau_{\rm cool}} f_e(r).$$

Cooling outside the star

$$\boldsymbol{F}_{\rm rad} = -K\boldsymbol{\nabla}T, \quad K = K_0 \rho^{-2} T^{6.5}.$$

Kramers opacity

$$\boldsymbol{F}_{\rm SGS} = -\chi_{\rm SGS}^{(1)} \rho \boldsymbol{\nabla} s', \quad s' = s - \overline{s}_t.$$

Subgrid-scale entropy diffusion

# M dwarf parameter study

MS M5 star: $M = 0.2 M_\odot, \quad R = 0.27 R_\odot, \quad L = 0.008 L_\odot$

| Run | $P_{\rm rot}$[days] | Ta[$10^8$] | $u_{\rm rms}$[m/s] | $B_{\rm rms}$[kG] | Co | Co$^{(\omega)}$ | Ra$_t$ | Re | Pe | Re$_M$ | $\tau_{\rm sim}$[years] | DR | grid |
|---|---|---|---|---|---|---|---|---|---|---|---|---|---|
| HD1 | – | – | 18 | – | – | – | $6.5\cdot10^5$ | 189 | 37 | – | 302 | – | $288^3$ |
| RHD1 | 433 | 0.16 | 17 | – | 0.6 | 0.1 | $2.3\cdot10^6$ | 181 | 36 | – | 58 | anti-solar | $288^3$ |
| RHD2 | 144 | 1.4 | 15 | – | 1.9 | 0.2 | $1.7\cdot10^6$ | 159 | 31 | – | 37 | solar-like | $288^3$ |
| RHD3 | 43 | 16 | 15 | – | 6.4 | 0.9 | $4.8\cdot10^6$ | 159 | 31 | – | 36 | solar-like | $288^3$ |
| RHD4 | 14 | 144 | 9.0 | – | 31 | 3.0 | $1.3\cdot10^7$ | 96 | 19 | – | 220 | solar-like | $288^3$ |
| RHD5 | 4.3 | 1600 | 5.7 | – | 166 | 11 | $7.9\cdot10^7$ | 61 | 12 | – | 209 | solar-like | $288^3$ |
| MHD0 | – | – | 18 | no dynamo | – | – | $6.5\cdot10^5$ | 189 | 37 | 95 | 87 | – | $288^3$ |
| MHD1 | 433 | 0.16 | 14 | 11 | 0.7 | 0.1 | $1.2\cdot10^6$ | 145 | 29 | 72 | 143 | anti-solar | $288^3$ |
| MHD1h | 433 | 1.4 | 14 | 12 | 0.7 | 0.1 | $3.6\cdot10^6$ | 293 | 58 | 146 | 79 | anti-solar | $576^3$ |
| MHD2 | 144 | 1.4 | 14 | 4.5 | 2.0 | 0.3 | $1.7\cdot10^6$ | 152 | 30 | 76 | 107 | solar-like | $288^3$ |
| MHD3 | 43 | 16 | 10 | 10 | 9.1 | 1.2 | $3.2\cdot10^6$ | 111 | 22 | 55 | 134 | solar-like | $288^3$ |
| MHD3h | 43 | 64 | 10 | 12 | 9.4 | 1.4 | $8.0\cdot10^6$ | 215 | 43 | 107 | 83 | solar-like | $576^3$ |
| MHD4 | 14 | 144 | 5.8 | 13 | 49 | 3.6 | $7.8\cdot10^6$ | 62 | 12 | 31 | 201 | solar-like | $288^3$ |
| MHD5 | 4.3 | 2500 | 2.6 | 19 | 366 | 24 | $1.1\cdot10^7$ | 34 | 6 | 17 | 302 | solar-like | $288^3$ |
| MHD5h | 4.3 | $10^4$ | 2.5 | 23 | 375 | 14 | $3.7\cdot10^7$ | 67 | 13 | 33 | 149 | solar-like | $576^3$ |

$$\mathrm{Co} = \frac{2\Omega_0}{u_{\rm rms} k_R}, \quad k_R = 2\pi/R. \qquad \mathrm{Pr_{SGS}} \equiv \frac{\nu}{\chi^{(1)}_{\rm SGS}} = 0.2, \quad \mathrm{Pr} \equiv \frac{\nu}{\chi} \gg 1, \quad \mathrm{Pr_M} \equiv \frac{\nu}{\eta} = 0.5.$$

$L_{\rm ratio} \approx 2.1 \cdot 10^9$

# Thermodynamic stratification

Deardorff layer $(\partial_r s > 0,\ F_{\rm conv} > 0.)$

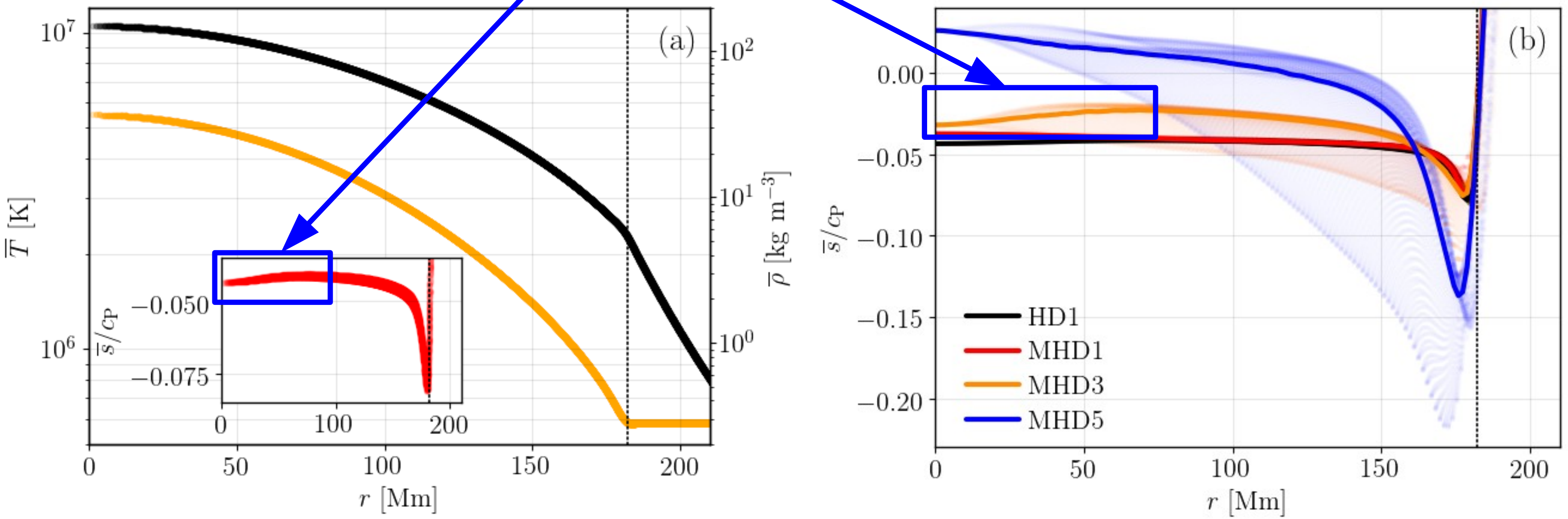

# (Hydrodynamic) Flow states

$\mathrm{non-rotating}$ $P_{\mathrm{rot}} = 433\ \mathrm{d}$ $P_{\mathrm{rot}} = 144\ \mathrm{d}$

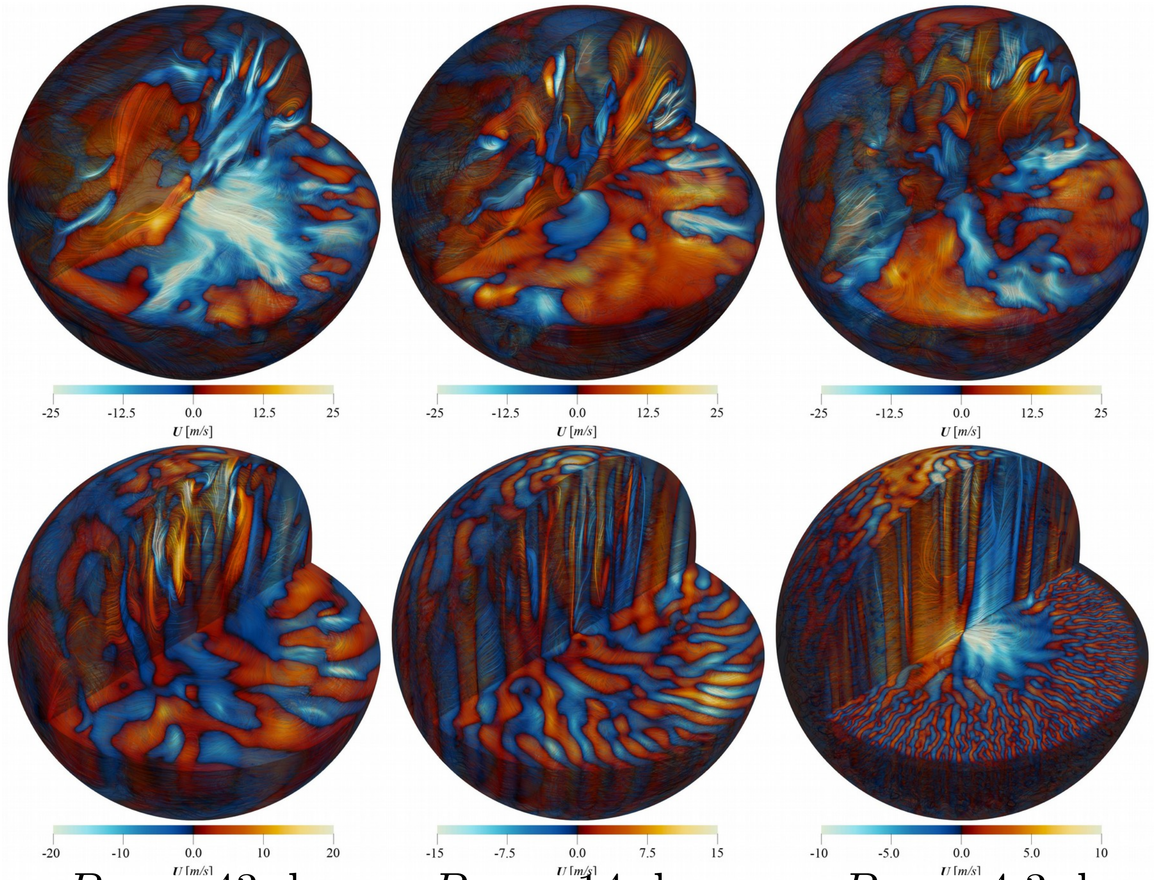


$P_{\mathrm{rot}} = 43\ \mathrm{d}$ $P_{\mathrm{rot}} = 14\ \mathrm{d}$ $P_{\mathrm{rot}} = 4.3\ \mathrm{d}$

# Differential rotation

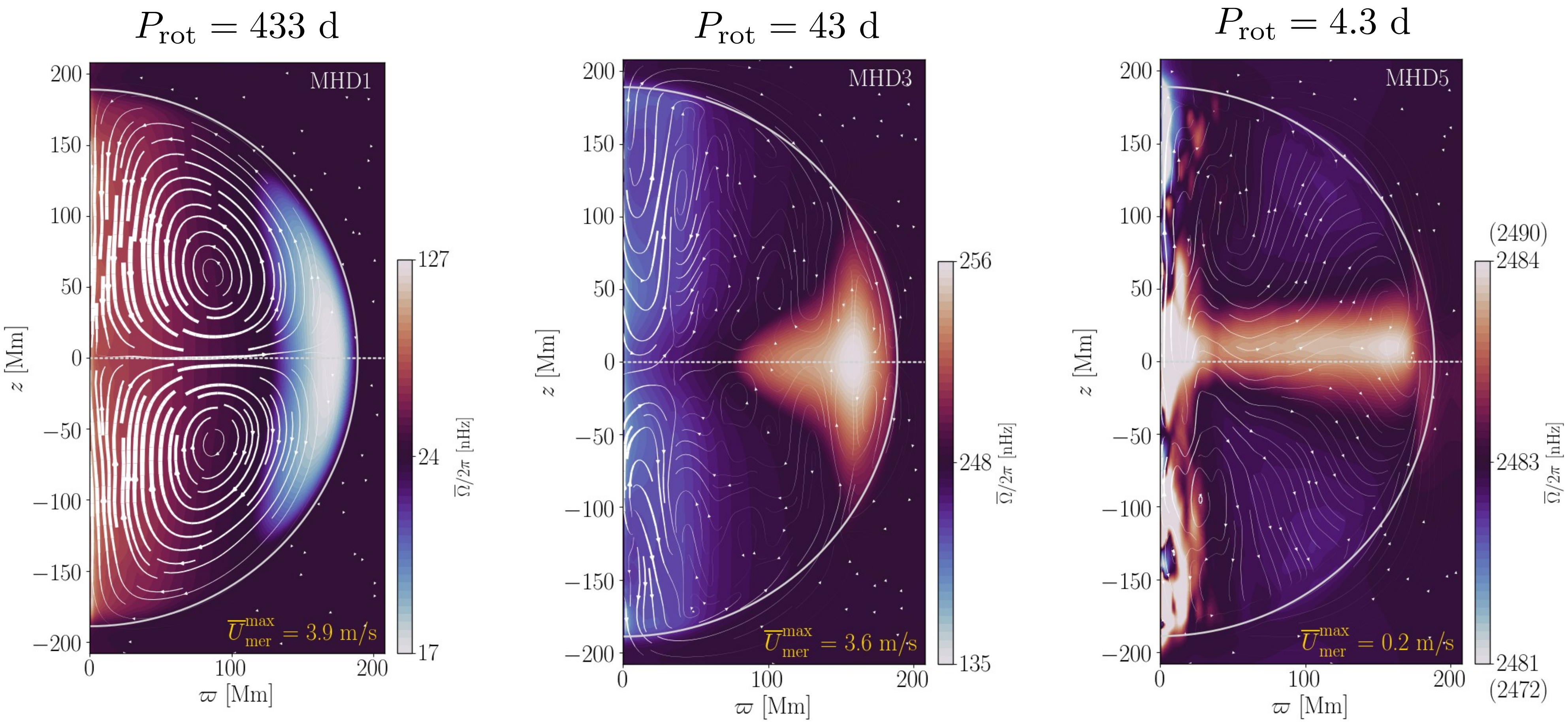


$$\overline{\Omega} = \overline{U}_\phi(r, z)/\varpi + \Omega_0.$$

# Slow rotation

$P_{\mathrm{rot}} = 433$ d

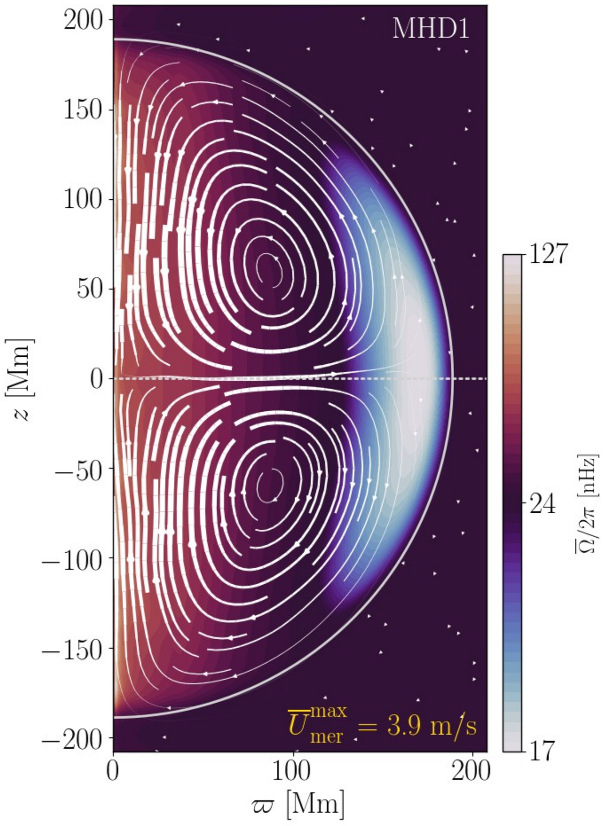


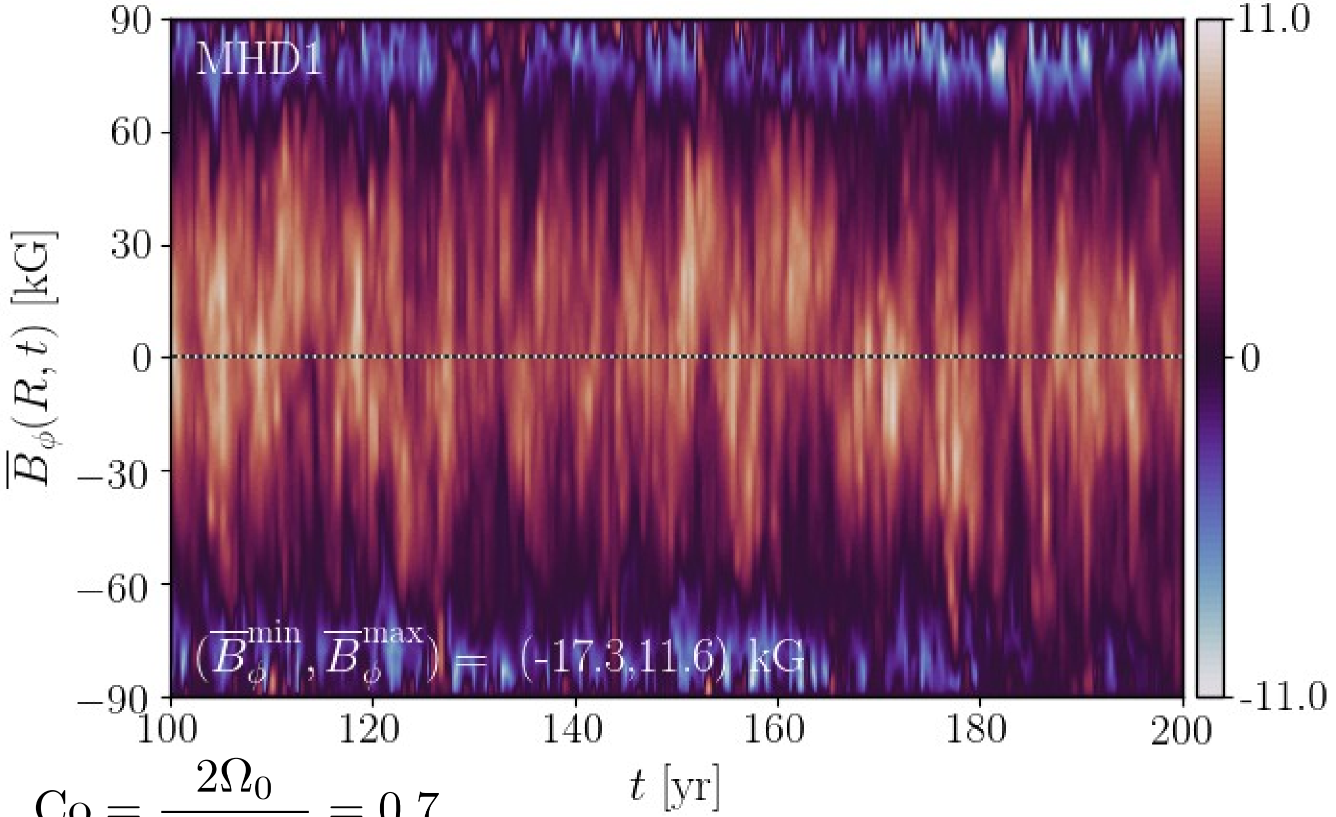


$$\mathrm{Co} = \frac{2\Omega_0}{u_{\mathrm{rms}} k_R} = 0.7$$

# Slow rotation

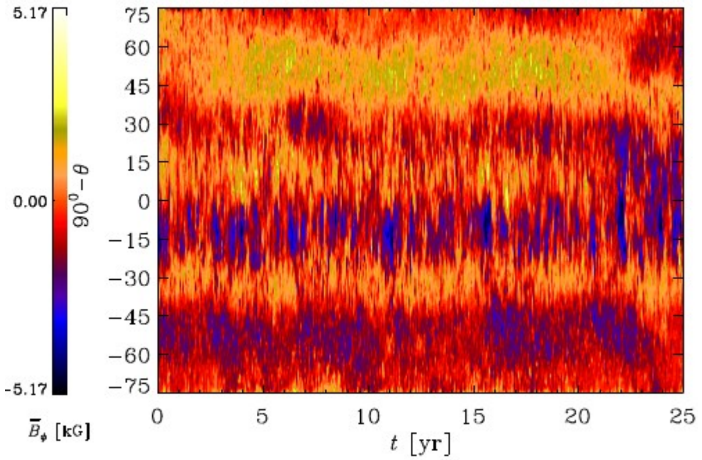


$$\mathrm{Co} = \frac{2\Omega_0}{u_{\mathrm{rms}} k_1} = 1.5,$$

$$\Delta R = 0.3 R_\odot.$$

$$k_1 = 2\pi/\Delta R,$$

(Käpylä et al. 2017, *A&A*, **599**, A4)

(Strugarek et al. 2018, *A&A*, **863**, 35)

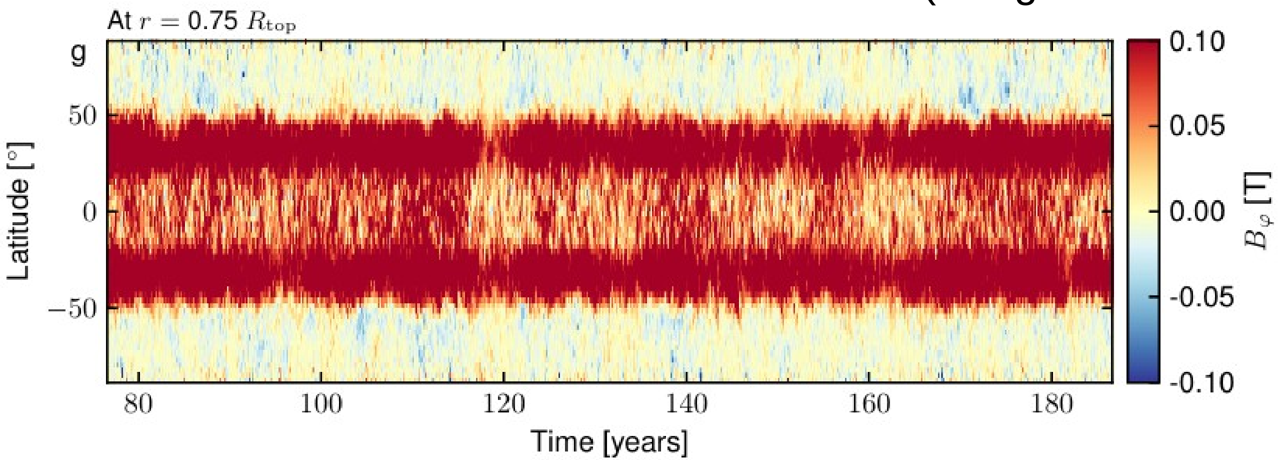


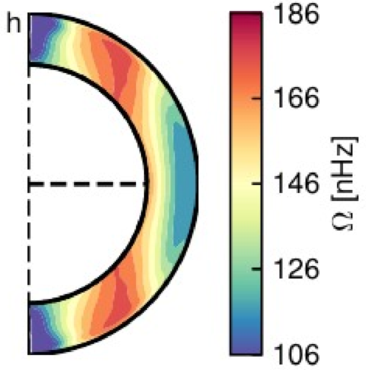


$$\Omega = \Omega_\odot/3$$

# Intermediate rotation

$P_{\rm rot} = 43$ d

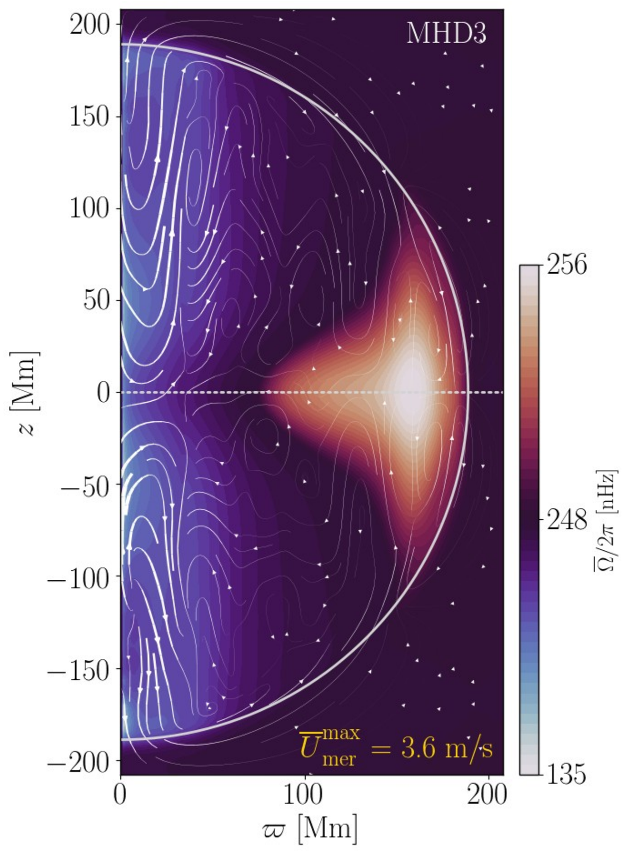


Gilman (1983), Glatzmaier (1985)...

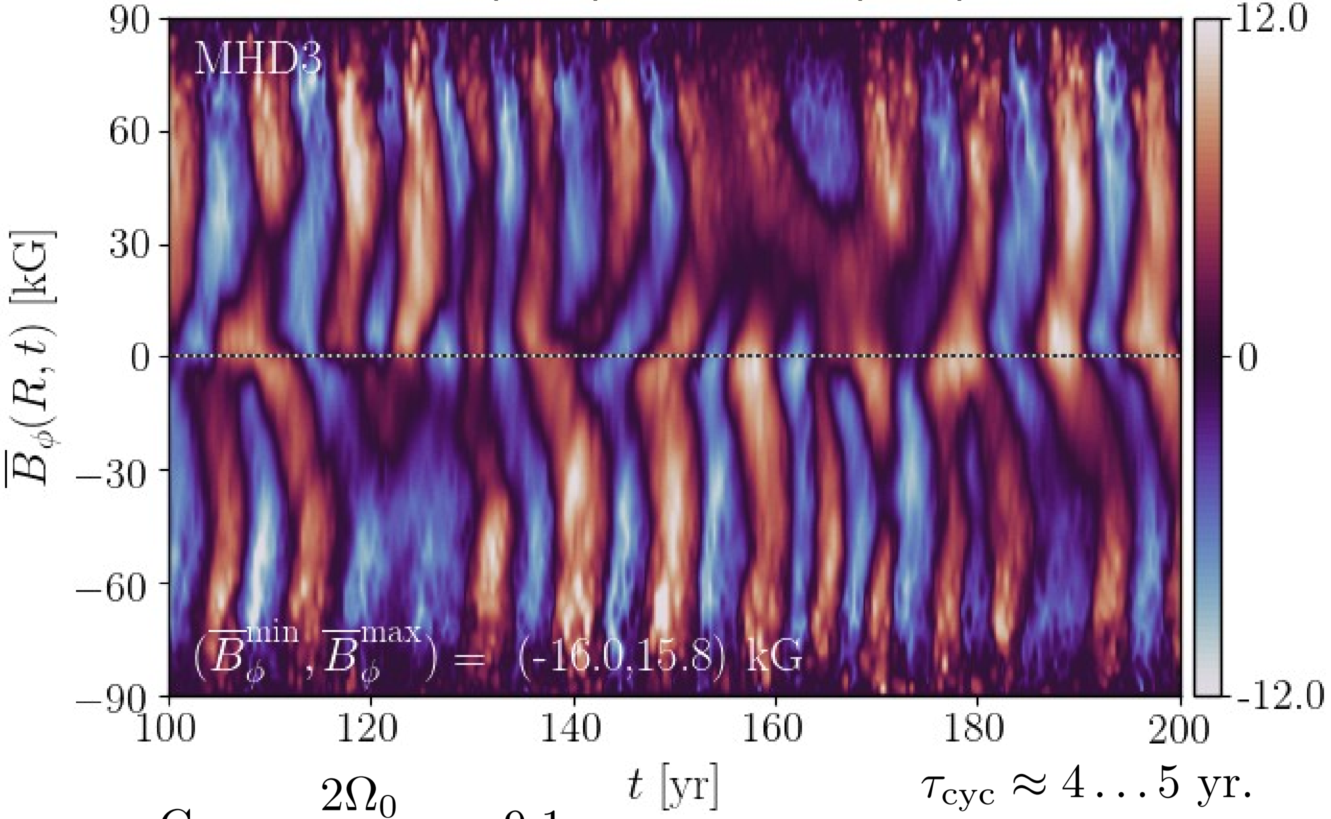


$\tau_{\rm cyc} \approx 4\ldots 5$ yr.

$$\mathrm{Co} = \frac{2\Omega_0}{u_{\rm rms}k_R} = 9.1$$

$$\mathrm{Ro}^{(\omega)} = \frac{\omega_{\rm rms}}{2\Omega_0} = 0.8$$

# Comparison to spherical simulations

THE ASTROPHYSICAL JOURNAL LETTERS, 902:L3 (6pp), 2020 October 10
https://doi.org/10.3847/2041-8213/abb9a4


CrossMark

## Single-hemisphere Dynamos in M-dwarf Stars

Benjamin P. Brown[1], Jeffrey S. Oishi[2], Geoffrey M. Vasil[3], Daniel Lecoanet[4], and Keaton J. Burns[5,6]
[1] Department Astrophysical and Planetary Sciences & LASP, University of Colorado, Boulder, CO 80309, USA; bpbrown@colorado.edu
[2] Department of Physics and Astronomy, Bates College, Lewiston, ME 04240, USA
[3] School of Mathematics and Statistics, University of Sydney, Sydney, NSW 2006, Australia
[4] Department of Engineering Science and Applied Mathematics, Northwestern University, 2145 Sheridan Road, Evanston, IL 60208, USA
[5] Department of Mathematics, Massachusetts Institute of Technology, Cambridge, MA 02139, USA
[6] Center for Computational Astrophysics, Flatiron Institute, New York, NY 10010, USA
*Received 2020 August 4; revised 2020 September 11; accepted 2020 September 17; published 2020 October 7*

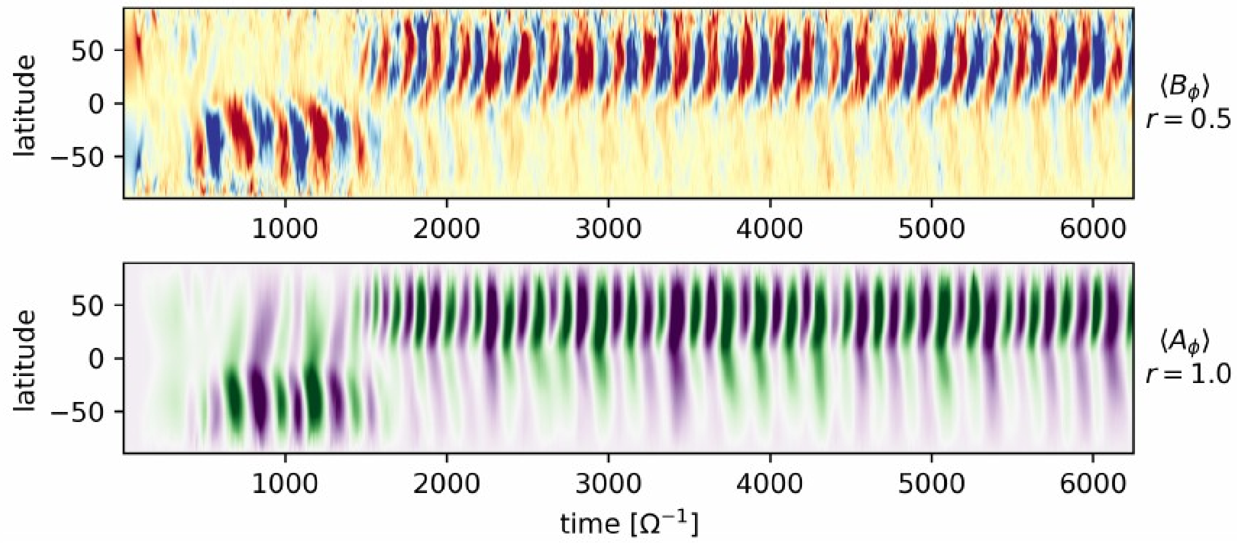


This Letter has focused on a single-dynamo solution that shows striking hemispheric asymmetries. We find the same preference for single-hemisphere dynamos in every fully convective M-dwarf case computed to present, including a sweep of cases at $\mathrm{Ek} = 2.5 \times 10^{-5}$ and $\mathrm{Ro_C} = 0.38$–$0.57$, corresponding to rms Reynolds numbers of 210–350 and Rossby numbers of 0.27–0.42. These cases also all undergo cyclic reversals of magnetic polarity. To check if single-hemisphere preference happens spuriously from a numerical source, we also rotated around the $\hat{\boldsymbol{x}}$ rather than the $\hat{z}$ axis (for $\mathrm{Ro_C} = 0.41$, $\mathrm{Ek} = 2.5 \times 10^{-5}$). In this strange solution, cycling single-hemispheric-dynamo action happened around the east–west pole, relative to the numerical grid.

# Comparison to spherical simulations

THE ASTROPHYSICAL JOURNAL LETTERS, 833:L28 (6pp), 2016 December 20
doi:10.3847/2041-8213/833/2/L28


CrossMark

MAGNETIC CYCLES IN A DYNAMO SIMULATION OF FULLY CONVECTIVE M-STAR PROXIMA CENTAURI

RAKESH K. YADAV[1], ULRICH R. CHRISTENSEN[2], SCOTT J. WOLK[1], AND KATJA POPPENHAEGER[3,1]
[1] Harvard-Smithsonian Center for Astrophysics, 60 Garden Street, Cambridge, MA 02138, USA; rakesh.yadav@cfa.harvard.edu
[2] Max-Planck-Institut für Sonnensystemforschung, Justus-von-Liebig-Weg 3, D-37077 Göttingen, Germany
[3] Astrophysics Research Center, Queen's University Belfast, Belfast BT7 1NN, UK
Received 2016 October 8; revised 2016 November 28; accepted 2016 December 1; published 2016 December 19

$\tau_{\rm cyc}/2 \approx 9$ yr.

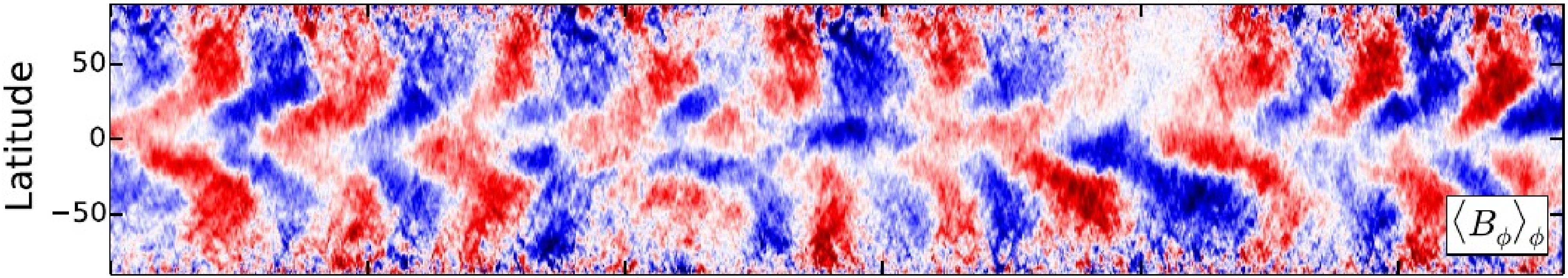


Observational results: e.g. Suárez Mascareno et al. (2016), Wargelin et al. (2017)...

# Rapid rotation

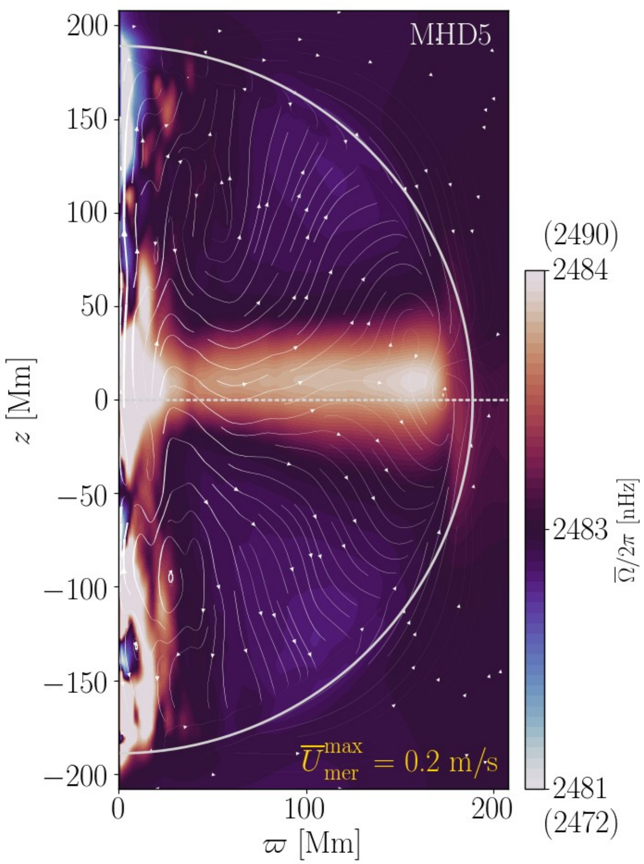


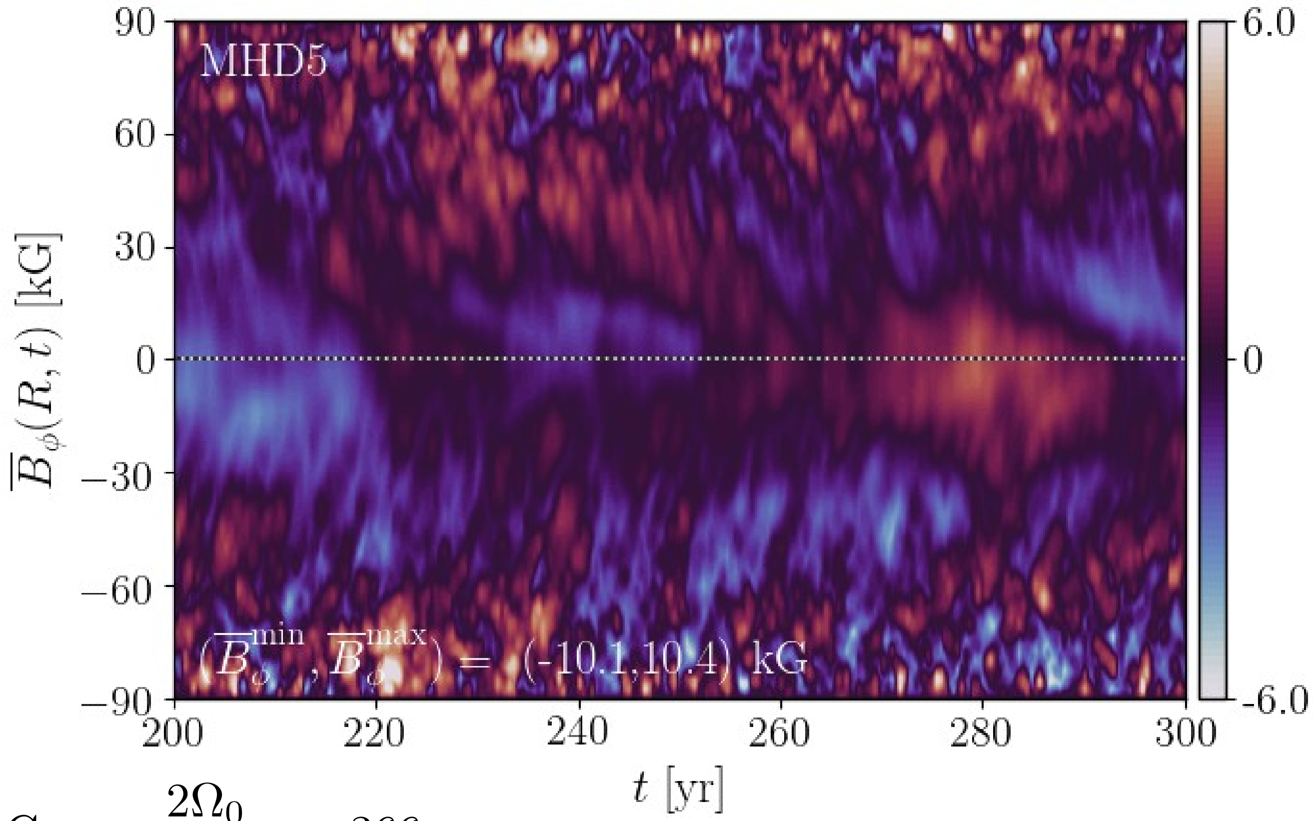


$$\mathrm{Co} = \frac{2\Omega_0}{u_{\rm rms} k_R} = 366.$$

# Rapid rotation

Velocity

Magnetic field (equator)

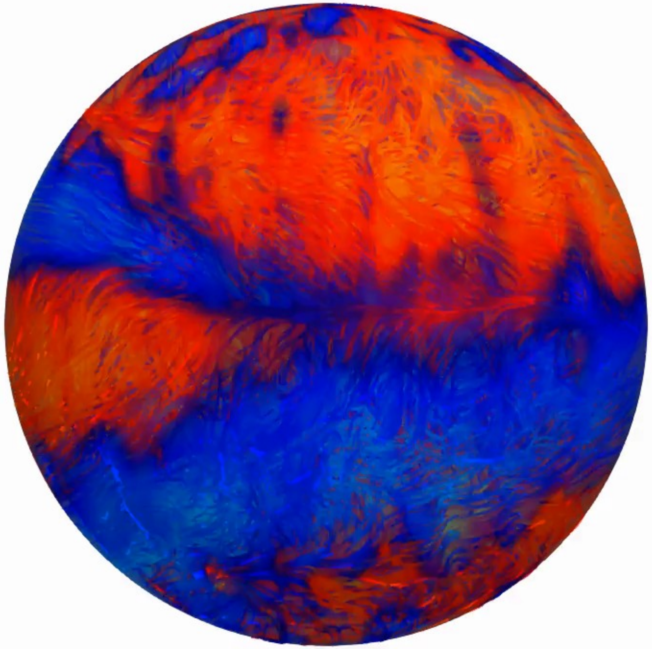

Magnetic field (pole)

The video covers about 40 years of evolution.

# Rapid rotation: azimuthal dynamo wave

View at the pole:

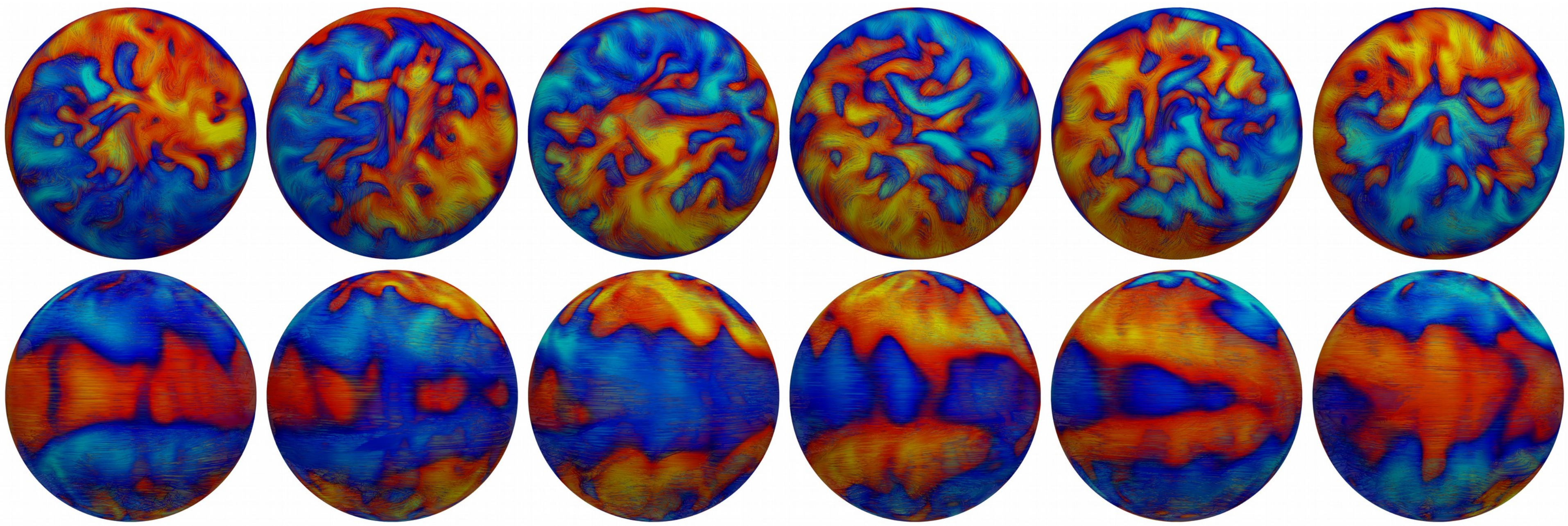

View at the equator:

(e.g. Krause & Rädler (1980), Cole et al. (2014), *Astrophys. J. Lett.*, **780**, 22; Viviani et al. (2018), *Astron. Astrophys.*, **616**, 160.)

# How about partially convective stars?

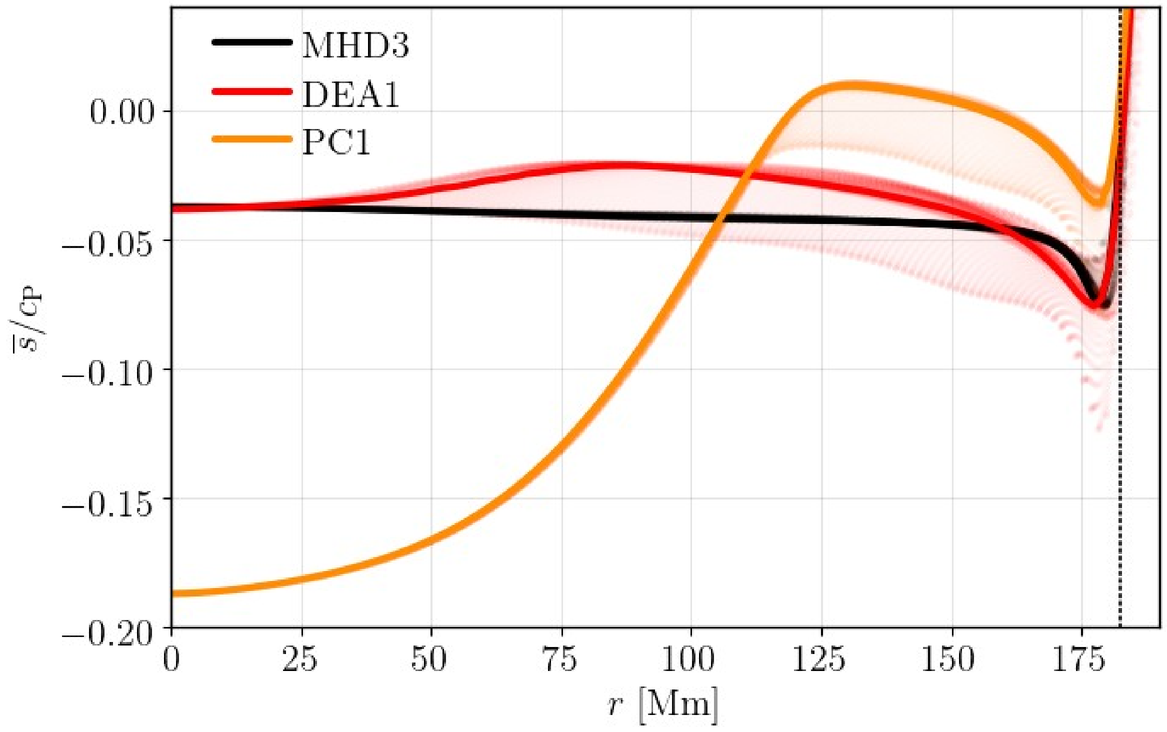


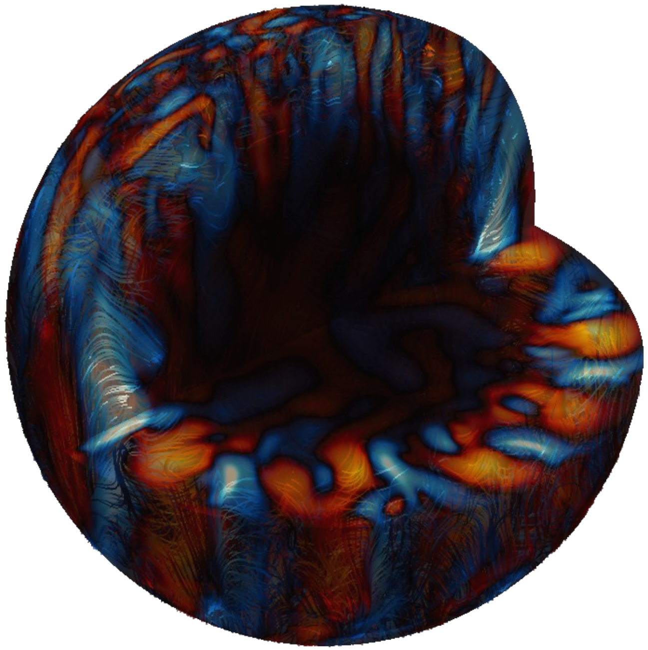

Three runs with same $P_{\mathrm{rot}}$, different $K_0$. $\boldsymbol{F}_{\mathrm{rad}} = -K\boldsymbol{\nabla}T, \quad K = K_0\rho^{-2}T^{6.5}$

# How about partially convective stars?

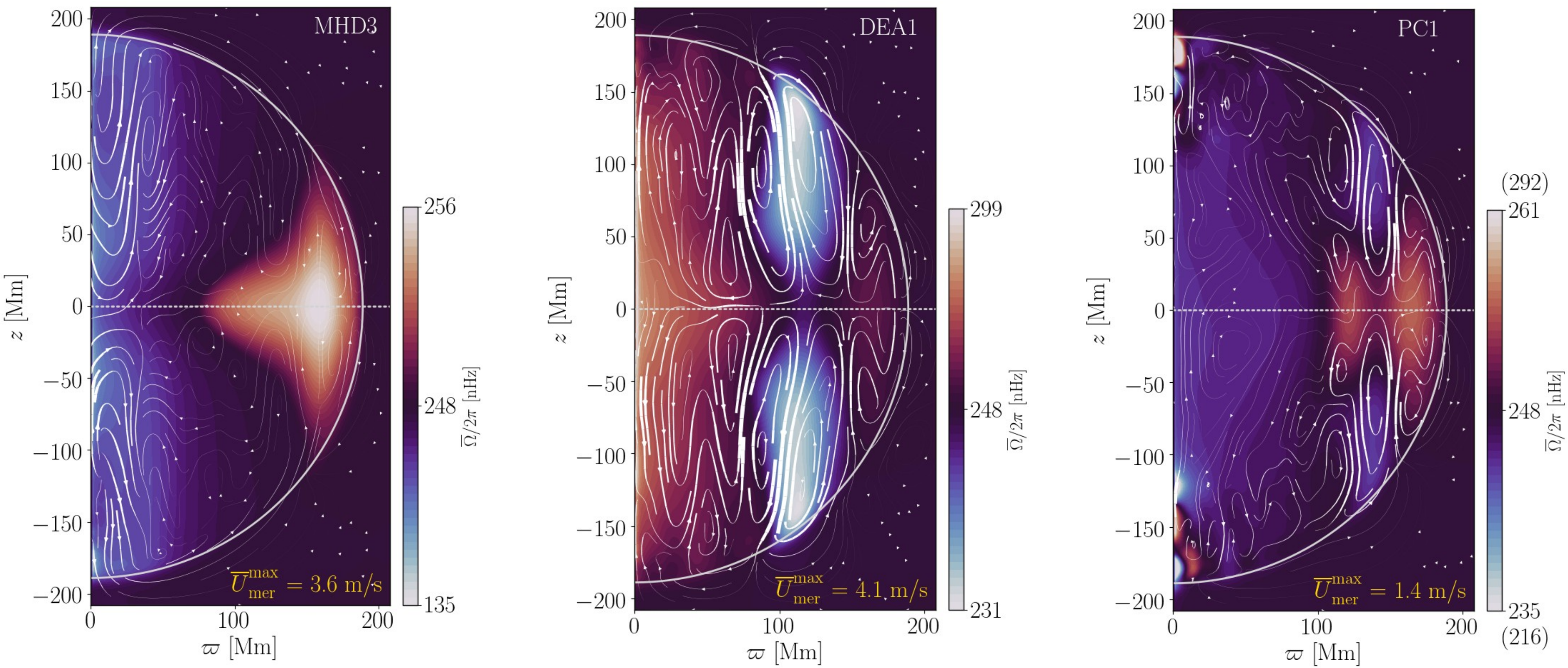


$P_{\rm rot} = 43$ d

Pencil Code User Meeting 20 May 2021

# How about partially convective stars?

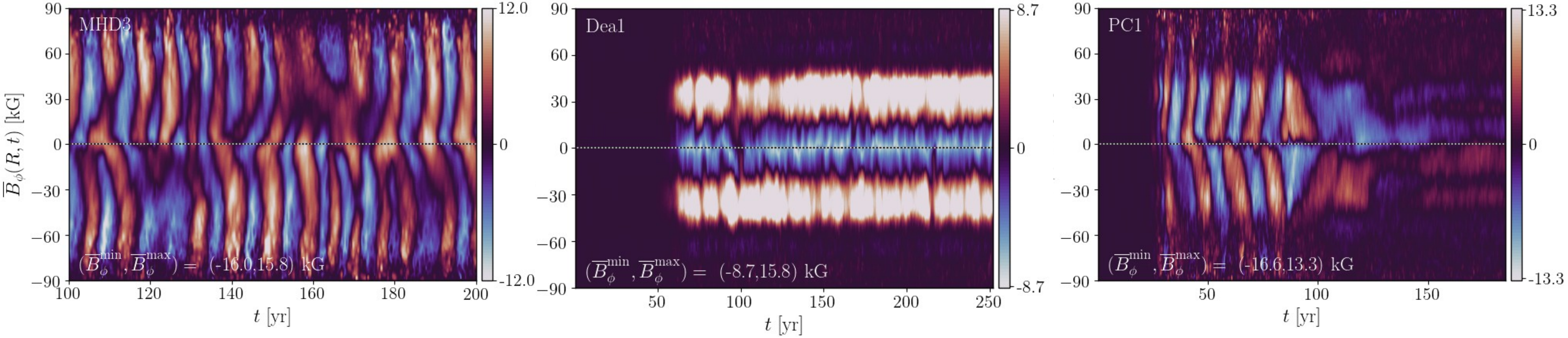


Cycles disappear in Deardorff and partially convective runs?

# How about partially convective stars?

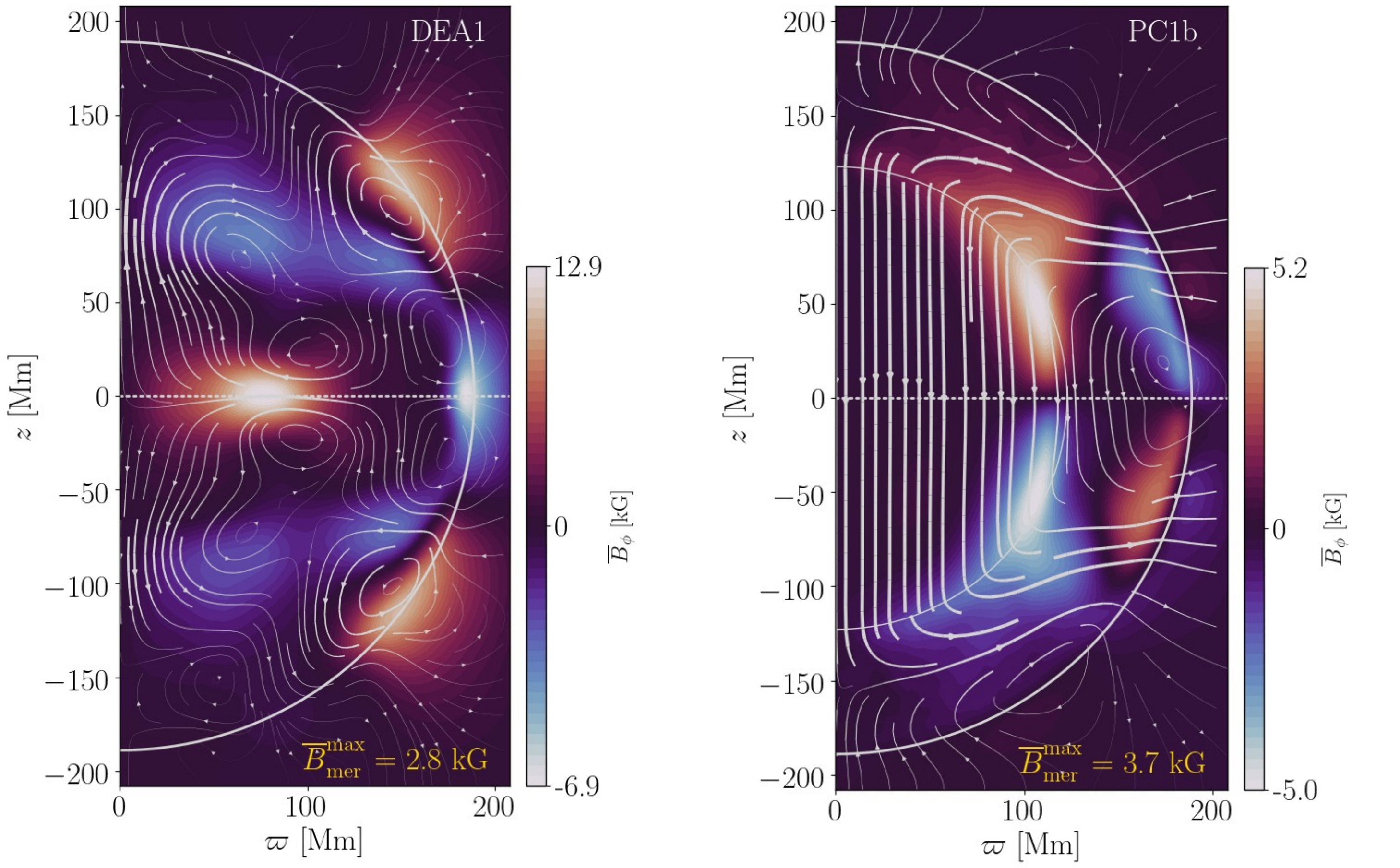

# Conclusions

- Transitions of differential rotation and magnetism occur similarly in partially and fully convective stars.
- Quasi-steady magnetic fields for slow rotation, cyclic and axisymmetric for intermediate rotation, and non-axisymmetric for rapid rotation.
- Future studies: more realistic flow regimes, self-gravity, radiation, magnetic braking.

# Transition to full convection

According to stellar structure and evolution models the transition occurs around $M = 0.35 M_\odot$.

Interestingly, the transition is not continuous: a minimum stable size of the radiative core is around $0.4 R_{\rm star}$.

(Jao et al. 2018, *Astrophys. J. Lett.*, **861**, 11; Baraffe & Chabrier 2018, *Astron. Astrophys.*, **619**, 177; Feiden et al. 2020, *arXiv:2020.07991*)

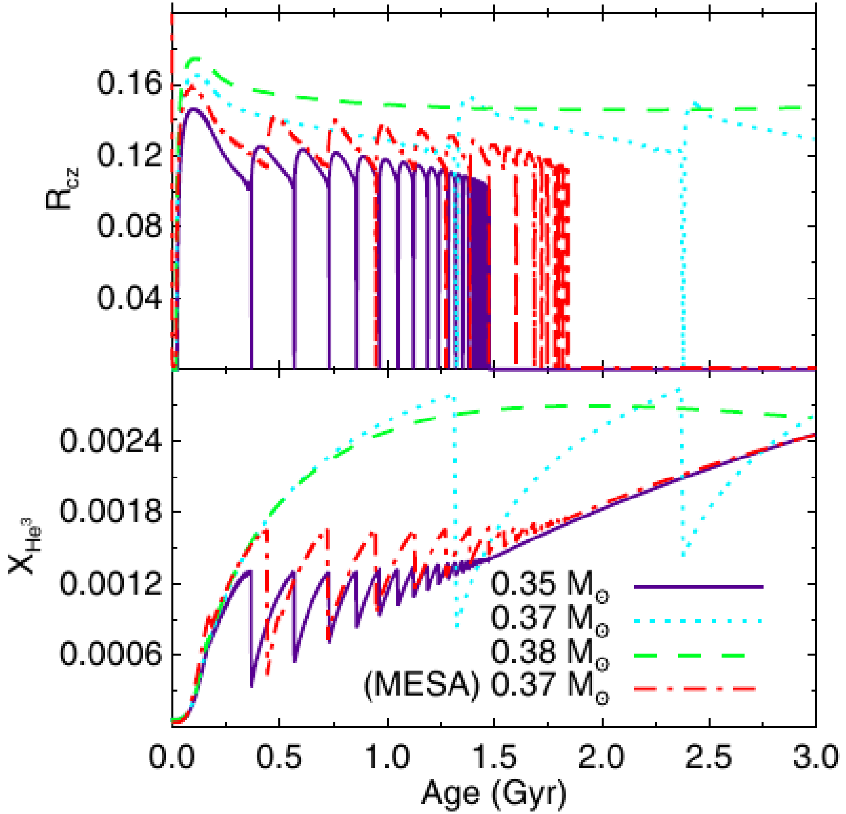


van Saders & Pinsonneault (2012), *Astrophys. J.*, **751**, 98

# Enhanced luminosity method

M stars have a low luminosity leading to slow convective velocities. Thus the Mach number is small:

$$\mathrm{Ma} = \frac{u_{\mathrm{conv}}}{c_{\mathrm{s}}} = 10^{-5} \ldots 10^{-2}, \; u_{\mathrm{conv}} \propto \left(\frac{L}{\rho}\right)^{1/3}.$$

Timestep of simulations determined by the fastest signal speed: $\delta t = \Delta x / \max(c_{\mathrm{s}}, u_{\mathrm{conv}}, v_{\mathrm{A}}, \ldots)$.

Typical values yield $\delta t_{\mathrm{ac}} \approx 1\,\mathrm{s}$. However, the Kelvin-Helmholtz time ($\tau_{\mathrm{KH}} = GM^2/RL$) in M stars is $10^9$-$10^{10}$ years.

The wall-clock time per timestep for a typical current simulation is roughly $0.1\mathrm{s}$ $\rightarrow$ time to solution $10^8$ ($10^3$) years.

# Enhanced luminosity method

Enhanced luminosity method (ELM): use a much higher luminosity in the simulation, $L = L_{\mathrm{ratio}} L_{\star},\ L_{\mathrm{ratio}} \gg 1.$

Reinterpret $u_{\mathrm{conv}}$ *as the actual convective velocity*. Implies rescaling of sound speed, $c_{\mathrm{s}} \propto L_{\mathrm{ratio}}^{-1/3}$ :

$$\mathrm{Ma}_{\mathrm{ELM}} = \frac{u_{\mathrm{conv}}}{c_{\mathrm{s}}} = L_{\mathrm{ratio}}^{1/3} \mathrm{Ma}_{\star}.$$

Gap between $\tau_{\mathrm{KH}}$ and $\delta t_{\mathrm{ac}}$ diminishes proportional to $L_{\mathrm{ratio}}^{4/3}$.

The model describes a numerically tractable analogy of the star where the range of timescales is compressed.